Doping a Correlated Band Insulator: A New Route to Half-Metallic Behavior

Arti Garg,[1] H. R. Krishnamurthy,[2] and Mohit Randeria[3]
[1]Condensed Matter Physics Division, Saha Institute of Nuclear Physics, 1/AF Bidhannagar, Kolkata 700 064, India
[2]Centre for Condensed Matter Theory, Department of Physics, Indian Institute of Science, Bangalore 560 012, India and JNCASR, Jakkur, Bangalore 560 064, India
[3]Department of Physics, The Ohio State University, Columbus, Ohio 43210, USA
(Received 23 July 2013; revised manuscript received 10 December 2013; published 12 March 2014)

We demonstrate in a simple model the surprising result that turning on an on-site Coulomb interaction U in a doped band insulator leads to the formation of a half-metallic state. In the undoped system, we show that increasing U leads to a first order transition at a finite value U_{AF} between a paramagnetic band insulator and an antiferomagnetic Mott insulator. Upon doping, the system exhibits half-metallic ferrimagnetism over a wide range of doping and interaction strengths on either side of U_{AF}. Our results, based on dynamical mean field theory, suggest a new route to half metallicity, and will hopefully motivate searches for new materials for spintronics.

DOI: 10.1103/PhysRevLett.112.106406 PACS numbers: 71.10.Fd, 71.10.Hf, 71.27.+a, 71.30.+h

Turning on strong electron correlations in a normal metal is expected to lead to interesting phases like Mott insulators, high T_c superconductors, magnets, and non-Fermi liquids. But the effect of correlations in band insulators is less explored. In this Letter we study the effects of an on-site Hubbard interaction U on a band insulator and find a new route to half metallicity, namely, that doping a correlated band insulator leads to a half-metallic (HM) ferrimagnet.

Half metals are an interesting class of materials where electrons with one spin polarization behave as in a metal while those with the opposite spin polarization behave as in an insulator. They have applications in spintronics as they can generate spin-polarized currents [1]. There have been earlier theoretical suggestions, mainly using density functional theory, predicting half-metallic ferrimagnetism and antiferromagnetism (i.e., with zero net magnetization) in various materials [2,3]. These include transition metal oxides (e.g., NiO and MnO) with cation vacancies on one of the sublattices [4], hole-doped octuple perovskite cuprates [5], double perovskites [6], Heusler and semi-Heusler alloys [3,7], etc. The first two of these correspond to doped Mott insulators, that is, materials that would have been metals if the correlations had been switched off. The last two mostly involve materials that contain both localized and itinerant spins. The mechanism presented here in our work, arising from doping a correlated band insulator, is, therefore, quite distinct from all of these.

Specifically, we study in this Letter a simple tight-binding model with two bands, arising from a staggered potential Δ on a bipartite lattice, in the presence of an on-site U. At half filling, when one band is filled and the other is empty, the $U = 0$ system is a paramagnetic band insulator (BI). When U is turned on antiferromagnetic (AF) order sets in at a first order phase transition for $U \geq U_{\mathrm{AF}}$. Upon doping, we show that the system exhibits HM ferrimagnetism over a range of doping and U values.

Intuitively the formation of a HM state in our work can be understood as follows. Due to the staggered potential, the gaps between the top of the valence band and the bottom of the conduction band for the two spin components in the antiferromagnetic insulator (AFI) phase are different, e.g., $Eg_{\downarrow} < Eg_{\uparrow}$. On low hole doping, in a rigid band picture, one would expect it to be energetically favorable to put all of the holes in the down spin band. This makes the $\downarrow$-band conducting while the $\uparrow$-band remains insulating, resulting in a HM phase. Similarly for $U < U_{\mathrm{AF}}$, consider the BI in the presence of a small staggered magnetic field $h \to 0$ such that the gap for the two spins is different, with $Eg_{\uparrow} = Eg + h$ and $Eg_{\downarrow} = Eg - h$. Doping this BI with x holes again results in a half metal, following the same reasoning as above, with a net moment $\sim x$, which, due to the molecular field arising from U, self-consistently leads to a staggered magnetization. The simple rigid band picture used in this argument is reasonable for small doping and weak coupling. We use dynamical mean field theory (DMFT) to address the following question: does the HM phase exists over a finite range of doping at intermediate and large U values? Our main results are summarized in the phase diagram of Fig. 1. We describe below in detail the spectral and magnetic properties that lead to this phase diagram, and show that the HM phase survives for the widest range of doping in the intermediate coupling regime where $U \sim 2\Delta$.

The model we use has tight-binding electrons on a bipartite lattice (sublattices A and B) described by

$$H = -t \sum_{i\in A, j\in B, \sigma} [c^{\dagger}_{i\sigma} c_{j\sigma} + \mathrm{H.c.}] - \mu \sum_i n_i + \Delta \sum_{i\in A} n_i - \Delta \sum_{i\in B} n_i + U \sum_i n_{i\uparrow} n_{i\downarrow}, \quad (1)$$

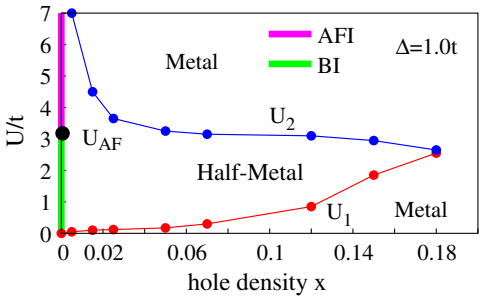

FIG. 1 (color online). $T = 0$ phase diagram of the model in Eq. (1) obtained within DMFT for the Bethe lattice of infinite connectivity. At half filling, the small-U band insulator becomes an AF insulator with a first order phase transition at U_{AF}. Upon doping, the system becomes a ferrimagnetic half metal.

where t is the nearest neighbor hopping, U is the Hubbard repulsion, and Δ is a staggered one-body potential that doubles the unit cell. The chemical potential μ is fixed so that the average occupancy is $(\langle n_A\rangle + \langle n_B\rangle)/2 = n = 1 - x$. The Hamiltonian (1) is sometimes called the "ionic Hubbard model" with Δ the "ionic" potential.

We have studied earlier the paramagnetic (PM) phases of this model, using DMFT with iterated perturbation theory (IPT) as the impurity solver. We showed that at half filling strong correlations close the gap in the BI leading to an intermediate metallic phase [8]. This result was reproduced qualitatively by other groups using other methods [9]. Here we study the model in Eq. (1) using the same DMFT + IPT approach, but now allowing for magnetic order. We show below that, at half filling, there is a first order phase transition from a PM BI to an AFI (see Fig. 1. We note that, unless the model is modified to introduce magnetic frustration, the AFI discussed here overwhelms the metallic phase [8] at half filling. The most unexpected results we report below are related to half-metallic behavior upon doping away from half filling. While previous authors have considered magnetic phases both at half filling [10] and away from it [11] in this model, to the best of our knowledge the existence of a half metal has not been suggested so far.

DMFT has been demonstrated to be successful in understanding the metal-insulator transition [12,13] in the usual Hubbard model, the $\Delta = 0$ limit of Eq. (1). We focus here on magnetic solutions of Eq. (1) for which it is convenient to introduce the matrix Green's function

$$\hat{G}^{\sigma}_{\alpha\beta}(\mathbf{k}, i\omega_n) = \begin{pmatrix} \zeta_{A\sigma}(i\omega_n) & -\epsilon_{\mathbf{k}} \\ -\epsilon_{\mathbf{k}} & \zeta_{B\sigma}(i\omega_n) \end{pmatrix}^{-1}, \qquad (2)$$

where α, β are sublattice (A, B) indices, σ is the spin index, $\mathbf{k}$ belongs to the first Brillouin zone of one sublattice, $i\omega_n = (2n+1)\pi T$, and T is the temperature. $\zeta_{A(B)\sigma} \equiv i\omega_n \mp \Delta + \mu - \Sigma_{A(B)\sigma}(i\omega_n)$, where the Σ's are the self-energies and $\epsilon_{\mathbf{k}}$ is the dispersion. DMFT includes local quantum fluctuations by mapping [12,13] the lattice problem onto a single-site or "impurity" with local interaction U hybridizing with a self-consistently determined bath. We use as our "impurity solver" a generalization of the IPT [12,14] scheme. Details of DMFT and generalized IPT are discussed in the Supplemental Material [15].

We present results for the $T = 0$ solution of DMFT equations on a Bethe lattice of connectivity $z \to \infty$, with $t \to t/\sqrt{z}$ to get a nontrivial limit. The bare density of states (DOS) is then given by $\rho_0(\epsilon) = \sqrt{4t^2 - \epsilon^2}/(2\pi t^2)$, which greatly simplifies the integrals involved in the DMFT self-consistent equations. Past experience suggests that the results will be qualitatively similar for other systems with a compact DOS.

Half filling.—It is useful to understand the half-filled case $x = 0$ before turning to the doped system. The left panel of Fig. 2 shows the staggered magnetization $m_s = (m_{zB} - m_{zA})/2$, where $m_{z\alpha} = n_{\uparrow\alpha} - n_{\downarrow\alpha}$ is the sublattice magnetization. For a given Δ, there exists a threshold value U_{AF} at which the staggered magnetization turns on with a jump at a first order phase transition. Due to the presence of the staggered potential, the AF instability does not occur at arbitrarily small U. Both U_{AF} and the jump in m_s at U_{AF} are increasing functions of Δ. Note that since at half filling $n_{A\sigma} + n_{B\sigma} = 1$, the uniform magnetization $m_F = n_\uparrow - n_\downarrow = (m_{zA} + m_{zB})/2 = 0$. The right panel of Fig. 2 shows the staggered occupancy $\delta n = (n_B - n_A)/2$, which is the difference in the filling of the two sublattices. Due to the staggered on-site potential, δn is always nonzero, even though the Hubbard U tries to suppress it. δn decreases monotonically as a function of U, and shows a discontinuity at U_{AF}.

Next we discuss the single particle DOS $\rho_\sigma(\omega) = -\sum_{k,\alpha} \mathrm{Im}\hat{G}^{\sigma}_{\alpha\alpha}(k, \omega^+)/\pi$, where σ is the spin, $\alpha = A, B$, and ω is measured from the chemical potential μ. The spectral gap $E_{g\sigma}$ in $\rho_\sigma(\omega)$ is shown in Fig. 3. For $U < U_{\mathrm{AF}}$, the spectral gap is the same for both of the spins due to the spin symmetry of the paramagnetic BI phase. In the BI, the gaps decrease with an increase in U/t. This is because U suppresses the effect of the staggered potential Δ,

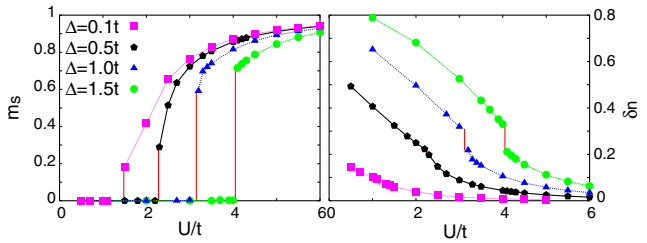

FIG. 2 (color online). Left panel: staggered magnetization m_s vs U/t for various Δ values. The onset of m_s marks a first order transition from a BI to an AFI at U_{AF}. Right panel: staggered occupancy $\delta n = (n_B - n_A)/2$ vs U/t for various Δ's. Although nonzero for all U/t, δn exhibits a discontinuity at U_{AF}. These results are for $n = 1$.

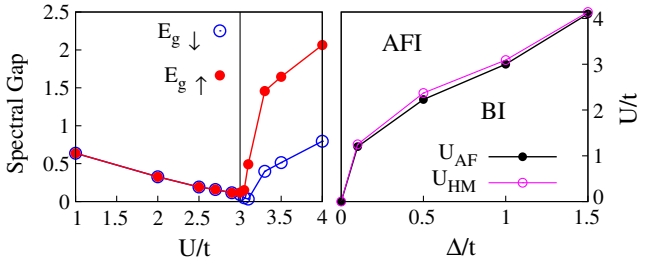

FIG. 3 (color online). Left panel: spin-resolved spectral gaps $E_{g\uparrow}$ and $E_{g\downarrow}$ vs U/t for $\Delta = 1.0t$ and $n = 1$. For $U < U_{AF}$, $E_{g\uparrow} = E_{g\downarrow}$. At $U = U_{AF}$, there is a jump separating the two gaps with $E_{g\downarrow} < E_{g\uparrow}$. For $U > U_{HM}$, in the AFI phase, both gaps increase with increasing U/t. Right panel: $T = 0$ phase diagram at half filling. A first order transition separates the PM BI from an AFI. There is a special line $U = U_{HM} > U_{AF}$, on which the system is a half metal.

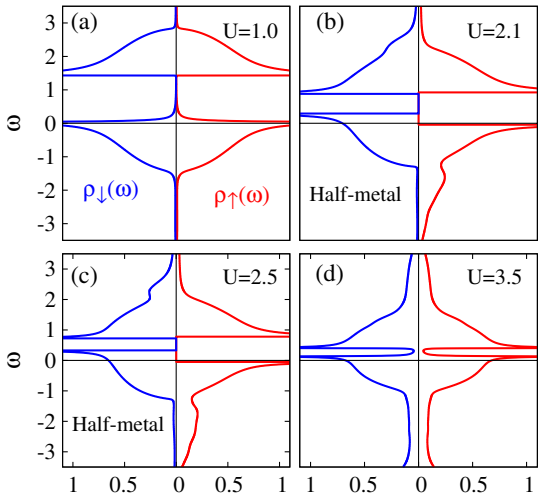

FIG. 4 (color online). Spin-resolved single particle DOS $\rho_\sigma(\omega)$ vs ω for $x = 0.17$ and $\Delta = t$. (a) Metallic phase for $U = t < U_1$ has spin symmetry with $\rho_\sigma(0) \neq 0$ for both spins. Half-metallic phase for $U_1 < U < U_2$ at (b) $U = 2.1t$ and (c) $U = 2.5t$ has $\rho_\uparrow(0) = 0$ while $\rho_\downarrow(0) \neq 0$. (d) Metal for $U = 3.5t > U_2$; the spin symmetry is restored with $\rho_\sigma(0) \neq 0$.

responsible for a nonzero gap. At $U = U_{AF}$, there occurs a jump separating the spectral gaps such that $E_{g\downarrow} < E_{g\uparrow}$. For $U > U_{AF}$, $E_{g\downarrow}$ keeps decreasing with increasing U and vanishes at $U_{HM} > U_{AF}$ while $E_{g\uparrow}$ starts increasing with an increase in U/t and stays nonzero at U_{HM}. Thus at half filling, we have a HM point at $U = U_{HM}$, details of which will be discussed elsewhere [16]. For $U > U_{HM}$, both of the gaps increase with an increase in U. The phase diagram in the (Δ, U) plane at half filling is shown in the right panel of Fig. 3. Note that the different spectral gaps for up and down spins, a key feature to get the HM phase, arise from the staggered potential Δ. We next show how this HM point at half filling, actually broadens out into a HM phase with doping.

Hole doping.—The phase diagram in the doped case has a broad ferrimagnetic HM phase for $U_1 < U < U_2$ and $x < x_{max}$, which is around 0.18 for $\Delta = 1.0t$; see Fig. 1. Now we discuss how we use the DOS and magnetization to determine the phase boundaries U_1 and U_2, which then automatically fixes x_{max}.

Density of states.—Figure 4 shows the single particle DOS $\rho_\sigma(\omega)$ for both of the spin components. For $U < U_1$, the DOS for both of the spins is the same. In this regime the system is a PM metal since the chemical potential lies inside the lower band for both of the spins; see Fig. 4(a). For $U > U_1$, magnetic order sets in making the gaps and the DOS different for the two spin components; see Figs. 4(b) and 4(c). The chemical potential lies inside the lower band for the down-spin component making $\rho_\downarrow(\omega = 0) \neq 0$, while the up-spin DOS $\rho_\uparrow(\omega = 0) = 0$ as shown in Fig. 5; hence, the system is a HM. Although not clearly visible in Figs. 4(b) and 4(c), the chemical potential lies above the top of the up-spin valence band in the HM phase; for the parameters shown in Figs. 4(b) and 4(c), the separation is $\sim 0.05t$ (see the Supplemental Material [15]). For $U > U_2$, the chemical potential lies inside the valence band for both of the spin components. This makes both of the spin components conducting, with equal density of up and down spins, and the system becomes a paramagnetic metal; see Fig. 4(d) [17].

Magnetization.—In addition to the spectral properties, the magnetic properties in Fig. 6 also show dramatic changes at the phase boundaries U_1 and U_2 in Fig. 1. For small U values, magnetic order is not favored. As U increases, a first order transition occurs at U_1 when both of the sublattices acquire nonzero magnetization m_{zA} and m_{zB} with a jump at U_1. Since the system is doped, these magnetizations are not equal and opposite to each other. This results in a nonzero staggered magnetization $m_s = (m_{zB} - m_{zA})/2$ as well as a nonzero uniform magnetization $m_F = (m_{zA} + m_{zB})/2$.

Within an extension of our formalism to finite temperatures, we can study the stability of the HM phase as a function of temperature, and we find that the HM phase can survive up to reasonably high $k_B T_c \sim t/4$ (see the Supplemental Material [15]).

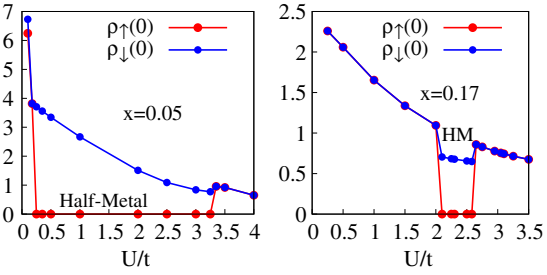

FIG. 5 (color online). Plot of $\rho_\sigma(\omega = 0)$ vs U/t for $x = 0.05$ and $x = 0.17$ at $\Delta = 1.0t$. At $x = 0.05$ there exists a broad HM phase in which $\rho_\uparrow(\omega = 0) = 0$ while $\rho_\downarrow(\omega = 0) \neq 0$. The width of the HM phase shrinks in U space as x increases.

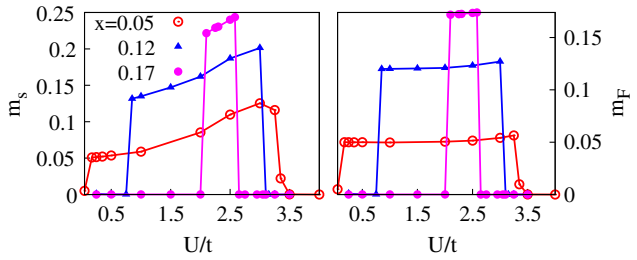

FIG. 6 (color online). Left panel: staggered magnetization m_s vs U/t. Right panel: uniform magnetization m_F vs U/t. At U_1 there is a discontinuous jump in both m_s and m_F making them nonzero. In the HM phase, $m_F \sim x$, as explained in the text. At U_2, both m_s and m_F drop to zero at another first order transition. $\Delta = 1.0t$ in both of the panels.

Within the HM phase m_F and m_s increase with increasing x. This is because, in the HM phase, the up-spin band is fully occupied implying $n_\uparrow = 1/2$ and all of the holes are doped in the down-spin band making $n_\downarrow = n - 1/2$. Therefore, the uniform magnetization m_F, which can also be written as $n_\uparrow - n_\downarrow$, goes as x and is independent of the interaction strength U/t. This is in agreement with our results in Fig. 6, within the numerical error bars. The staggered magnetization m_s, however, increases with increasing U/t. At $U_2 > U_1$ there occurs another first order transition and the system becomes a paramagnetic metal with both $m_F = m_s = 0$ for $U > U_2$.

It is important to ask how the size of the HM ferrimagnetic phase depends on the staggered potential, since Fig. 1 shows the result for a fixed Δ. We see in Fig. 7 that the width of the HM phase with doping x is largest for $U \sim 2\Delta$ and increases with an increase in Δ. This suggests that one should look for correlated band insulators with a large band gap, and an appropriately larger U, that can be doped readily, to find a robust HM phase.

Finally, it is interesting to compare our DMFT phase diagram with the phase diagram within the Hartree-Fock (HF) theory, details of which will be published elsewhere [16]. One can get a HM phase within a HF theory, but it overestimates the tendency to the formation of the half metal, and also predicts qualitatively wrong results. Within the HF theory for all $U > U_1$, the system is a half metal, the reason being the lack of quantum fluctuations in the HF theory, which are captured within DMFT.

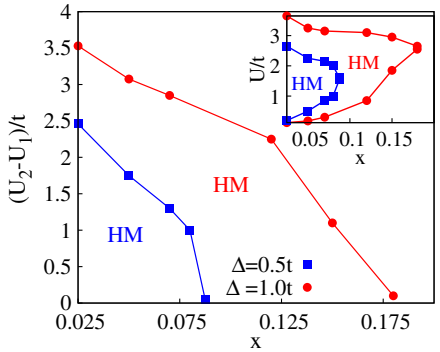

FIG. 7 (color online). The width $(U_2 - U_1)/t$ of the HM phase as a function of hole doping x. Inset: phase boundaries of the HM phase for $\Delta = 1.0t$ and $0.5t$. The HM phase, which lies in the area enclosed by the red dots (blue squares) for $\Delta = 1.0t(0.5t)$ gets wider with increase in Δ.

Conclusions—In conclusion, we have presented in this Letter a new mechanism whereby doping a correlated band insulator leads to a HM ferrimagnet. We emphasize that this mechanism is quite distinct from the mechanisms in well-known materials that exhibit this phenomenon like the manganites, double perovskites, or Heusler alloys, all of which have both local moments and itinerant electrons. Recently, there have been other theoretical discussions of HM behavior as well [18]. However, in all of these works either the HM phase exists only for some special doping values or it requires an external electric or magnetic field. The HM phase we discuss exists for a broad range of doping and is not dependent on application of external fields.

Although our finding is based on the study of a specific model, it suggests that for any correlated band insulator where the AFM phase at half filling is such that the up and down spins are at inequivalent sites with different local potentials, leading to different spectral gaps for the two spin components, and the AFM order survives on doping (more likely for correlated band insulators than for correlated metals), one should expect to see a HM phase upon doping. We hope that our study will motivate a search for materials along these lines and open up new possibilities in the area of spintronics.

M. R. would like to acknowledge support from DOE-BES DE-SC0005035; his collaboration with H. R. K. was made possible by NSF MRSEC DMR-0820414. H. R. K. would like to acknowledge support from the DST, India.

[1] W. E. Pickett and J. S. Moodera, Phys. Today **54**, 39 (2001); M. I. Katnelson, V. Y. Irkhin, L. Chioncel, and R. A. de Groot, Rev. Mod. Phys. **80**, 315 (2008); *Half-Metallic Alloys: Fundamentals and Applications*, Lecture Notes in Physics, edited by (Springer, New York. 2005), Vol. 676.
[2] W. E. Pickett and H. Eschrig, J. Phys. Condens. Matter **19**, 315203 (2007); Xiao Hu, Adv. Mater. **24**, 294 (2012).
[3] I. Galankis, K. Ozdogan, E. Sasioglu and B. Aktas, Phys. Status Solidi A **205**, 1036 (2008).
[4] D. Kodderitzsch, W. Hergert, Z. Szotek, and W. M. Temmerman, Phys. Rev. B **68**, 125114 (2003); W. B. Zhang, N. Yu. W. Y. Yu, and B. Y. Tang, Eur. Phys. J. B **64**, 153 (2008).
[5] Y. M. Nie, and X. Hu, Phys. Rev. Lett. **100**, 117203 (2008).
[6] W. E. Pickett, Phys. Rev. B **57**, 10613 (1998); D. D. Sarma, P. Mahadevan, T. Saha-Dasgupta, S. Ray, and A. Kumar, Phys. Rev. Lett. **85**, 2549 (2000); J. H. Park, S. K. Kwon, and B. I. Min, Phys. Rev. B **65**, 174401 (2002); O. Erten,

O. N. Meetei, A. Mukherjee, M. Randeria, N. Trivedi, and P. Woodward, Phys. Rev. Lett. **107**, 257201 (2011); Si-Da Li, P. Chen, and Band-Gui Liu, AIP Adv. **3**, 012107 (2013).

[7] R. A. de Groot, A. M. van der Kraan, and K. H. J. Buschow, J. Magn. Magn. Mater. **61**, 330 (1986); R. A. de Groot, Physica (Amsterdam) **172B**, 45 (1991); H. van Leuken, and R. A. de Groot, Phys. Rev. Lett. **74**, 1171 (1995).

[8] A. Garg, H. R. Krishnamurthy, and M. Randeria, Phys. Rev. Lett. **97**, 046403 (2006).

[9] L. Craco, P. Lombardo, R. Hayn, G. I. Japaridze and E. Muller-Hartmann, Phys. Rev. B **78**, 075121 (2008); N. Paris, K. Bouadim, F. Hebert, G. G. Batrouni, and R. T. Scalettar, Phys. Rev. Lett. **98**, 046403 (2007); A. T. Hoang, J. Phys. Condens. Matter **22**, 095602 (2010).

[10] S. S. Kancharla and E. Dagotto, Phys. Rev. Lett. **98**, 016402 (2007); K. Byczuk, M. Sekania, W. Hofstetter, and A. P. Kampf, Phys. Rev. B **79**, 121103 (2009).

[11] K. Bouadim, N. Paris, F. Hebert, G. G. Batrouni and R. T. Scalettar, Phys. Rev. B, **76**, 085112 (2007).

[12] A. Georges, G. Kotliar, W. Krauth, and M. J. Rozenberg, Rev. Mod. Phys. **68**, 13 (1996).

[13] T. Pruschke, M. Jarrell, and J. K. Freericks, Adv. Phys. **44**, 187 (1995).

[14] H. Kajueter and G. Kotliar, Phys. Rev. Lett. **77**, 131 (1996).

[15] See Supplemental Material at http://link.aps.org/supplemental/10.1103/PhysRevLett.112.106406 for a brief description of the DMFT and IPT methodology used and some additional results, including finite temperature effects.

[16] A. Garg, H. R. Krishnamurthy, and M. Randeria, (unpublished).

[17] Note that there is still a small band gap (but it lies at energies higher then μ). At even larger values of U, this gap will open up again separating the lower and the upper Hubbard band with the chemical potential being inside the lower Hubbard band.

[18] R. Nandkishore, G. W. Chern, and A. V. Chubukov, Phys. Rev. Lett. **108**, 227204 (2012); Z. Hao, and O. A. Starykh, Phys. Rev. B **87**, 161109(R) (2013); J. Yuan, D. Xu, H. Wang, Y. Zhou, J. Gao, and F. Zhang, Phys. Rev. B **88**, 201109(R) (2013).